16. STRUCTURE FUNCTIONS

Written Summer 2001 by B. Foster (University of Bristol), A.D. Martin (University of Durham), M.G. Vincter (University of Alberta). Updated Summer 2003.

16.1. Deep inelastic scattering

High energy lepton-nucleon scattering (deep inelastic scattering) plays a key role in determining the partonic structure of the proton. The process $\ell N \to \ell' X$ is illustrated in Fig. 16.1. The filled circle in this figure represents the internal structure of the proton which can be expressed in terms of structure functions.
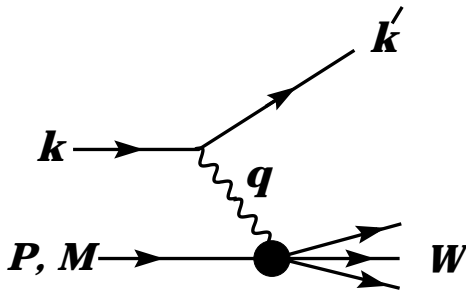

Figure 16.1: Kinematic quantities for the description of deep inelastic scattering. The quantities k and k' are the four-momenta of the incoming and outgoing leptons, P is the four-momentum of a nucleon with mass M, and W is the mass of the recoiling system X. The exchanged particle is a γ, $W^{\pm}$, or Z; it transfers four-momentum $q = k - k'$ to the nucleon.

Invariant quantities:

$\nu = \dfrac{q \cdot P}{M} = E - E'$ is the lepton's energy loss in the nucleon rest frame (in earlier literature sometimes $\nu = q \cdot P$). Here, E and E' are the initial and final lepton energies in the nucleon rest frame.

$Q^2 = -q^2 = 2(EE' - \vec{k} \cdot \vec{k}') - m_\ell^2 - m_{\ell'}^2$ where $m_\ell(m_{\ell'})$ is the initial (final) lepton mass. If $EE' \sin^2(\theta/2) \gg m_\ell^2, m_{\ell'}^2$, then

$\approx 4EE' \sin^2(\theta/2)$, where θ is the lepton's scattering angle in the nucleon rest frame with respect to the lepton beam direction.

$x = \dfrac{Q^2}{2M\nu}$ where, in the parton model, x is the fraction of the nucleon's momentum carried by the struck quark.

$y = \dfrac{q \cdot P}{k \cdot P} = \dfrac{\nu}{E}$ is the fraction of the lepton's energy lost in the nucleon rest frame.

$W^2 = (P + q)^2 = M^2 + 2M\nu - Q^2$ is the mass squared of the system X recoiling against the scattered lepton.

$s = (k + P)^2 = \dfrac{Q^2}{xy} + M^2 + m_\ell^2$ is the center-of-mass energy squared of the lepton-nucleon system.

2   *16. Structure functions*

The process in Fig. 16.1 is called deep ($Q^2 >> M^2$) inelastic ($W^2 >> M^2$) scattering (DIS). In what follows, the masses of the initial and scattered leptons, m_ℓ and m'_ℓ, are neglected.

16.1.1.   *DIS cross sections*:

$$\frac{d^2\sigma}{dx\,dy} = x\,(s - M^2)\,\frac{d^2\sigma}{dx\,dQ^2} = \frac{2\pi\,M\nu}{E'}\,\frac{d^2\sigma}{d\Omega_{\mathrm{Nrest}}\,dE'} \ . \tag{16.1}$$

In lowest-order perturbation theory, the cross section for the scattering of polarised leptons on polarised nucleons can be expressed in terms of the products of leptonic and hadronic tensors associated with the coupling of the exchanged bosons at the upper and lower vertices in Fig. 16.1 (see Refs. 1–4)

$$\frac{d^2\sigma}{dxdy} = \frac{2\pi y\alpha^2}{Q^4}\,\sum_j \eta_j\,L_j^{\mu\nu}\,W_{\mu\nu}^j \ . \tag{16.2}$$

For neutral-current processes, the summation is over $j = \gamma, Z$ and γZ representing photon and Z exchange and the interference between them, whereas for charged-current interactions there is only W exchange, $j = W$. (For transverse nucleon polarization, there is a dependence on the azimuthal angle of the scattered lepton.) $L_{\mu\nu}$ is the lepton tensor associated with the coupling of the exchange boson to the leptons. For incoming leptons of charge $e = \pm 1$ and helicity $\lambda = \pm 1$,

$$L_{\mu\nu}^\gamma = 2\left(k_\mu k'_\nu + k'_\mu k_\nu - k\cdot k' g_{\mu\nu} - i\lambda\varepsilon_{\mu\nu\alpha\beta}k^\alpha k'^\beta\right),$$

$$L_{\mu\nu}^{\gamma Z} = (g_V^e + e\lambda g_A^e)\,L_{\mu\nu}^\gamma, L_{\mu\nu}^Z = (g_V^e + e\lambda g_A^e)^2\,L_{\mu\nu}^\gamma,$$

$$L_{\mu\nu}^W = (1 + e\lambda)^2\,L_{\mu\nu}^\gamma, \tag{16.3}$$

where $g_V^e = -\frac{1}{2} - 2e\sin^2\theta_W$, $\qquad g_A^e = -\frac{1}{2}$.

Although here the helicity formalism is adopted, an alternative approach is to express the tensors in Eq. (16.3) in terms of the polarization of the lepton.

The factors η_j in Eq. (16.2) denote the ratios of the corresponding propagators and couplings to the photon propagator and coupling squared

$$\eta_\gamma = 1 \quad ; \quad \eta_{\gamma Z} = \left(\frac{G_F M_Z^2}{2\sqrt{2}\pi\alpha}\right)\left(\frac{Q^2}{Q^2 + M_Z^2}\right);$$

$$\eta_Z = \eta_{\gamma Z}^2 \quad ; \quad \eta_W = \frac{1}{2}\left(\frac{G_F M_W^2}{4\pi\alpha}\,\frac{Q^2}{Q^2 + M_W^2}\right)^2 . \tag{16.4}$$

The hadronic tensor, which describes the interaction of the appropriate electroweak currents with the target nucleon, is given by

$$W_{\mu\nu} = \frac{1}{4\pi}\int d^4 z\,e^{iq\cdot z}\,\left\langle P, S\left|\left[J_\mu^\dagger(z), J_\nu(0)\right]\right|P, S\right\rangle, \tag{16.5}$$

where S denotes the nucleon-spin 4-vector, with $S^2 = -M^2$ and $S\cdot P = 0$.

16.2.   Structure functions of the proton

The structure functions are defined in terms of the hadronic tensor (see Refs. 1–3)

$$
W_{\mu\nu} = \left(-g_{\mu\nu} + \frac{q_\mu q_\nu}{q^2} \right) F_1(x, Q^2) + \frac{\hat{P}_\mu \hat{P}_\nu}{P \cdot q} F_2(x, Q^2)
$$

$$
- i\varepsilon_{\mu\nu\alpha\beta} \frac{q^\alpha P^\beta}{2P \cdot q} F_3(x, Q^2)
$$

$$
+ i\varepsilon_{\mu\nu\alpha\beta} \frac{q^\alpha}{P \cdot q} \left[S^\beta g_1(x, Q^2) + \left(S^\beta - \frac{S \cdot q}{P \cdot q} P^\beta \right) g_2(x, Q^2) \right]
$$

$$
+ \frac{1}{P \cdot q} \left[\tfrac{1}{2} \left(\hat{P}_\mu \hat{S}_\nu + \hat{S}_\mu \hat{P}_\nu \right) - \frac{S \cdot q}{P \cdot q} \hat{P}_\mu \hat{P}_\nu \right] g_3(x, Q^2)
$$

$$
+ \frac{S \cdot q}{P \cdot q} \left[\frac{\hat{P}_\mu \hat{P}_\nu}{P \cdot q} g_4(x, Q^2) + \left(-g_{\mu\nu} + \frac{q_\mu q_\nu}{q^2} \right) g_5(x, Q^2) \right] \tag{16.6}
$$

where

$$
\hat{P}_\mu = P_\mu - \frac{P \cdot q}{q^2} q_\mu, \qquad \hat{S}_\mu = S_\mu - \frac{S \cdot q}{q^2} q_\mu . \tag{16.7}
$$

In Ref. 2, the definition of $W_{\mu\nu}$ with $\mu \leftrightarrow \nu$ is adopted, which changes the sign of the $\varepsilon_{\mu\nu\alpha\beta}$ terms in Eq. (16.6), although the formulae given here below are unchanged. Ref. 1 tabulates the relation between the structure functions defined in Eq. (16.6) and other choices available in the literature.

The cross sections for neutral and charged-current deep inelastic scattering on unpolarized nucleons can be written in terms of the structure functions in the generic form

$$
\frac{d^2\sigma^i}{dxdy} = \frac{4\pi\alpha^2}{xyQ^2} \eta^i \left\{ \left(1 - y - \frac{x^2 y^2 M^2}{Q^2} \right) F_2^i \right.
$$

$$
\left. + y^2 x F_1^i \mp \left(y - \frac{y^2}{2} \right) x F_3^i \right\}, \tag{16.8}
$$

where $i = $ NC, CC corresponds to neutral-current ($eN \to eX$) or charged-current ($eN \to \nu X$ or $\nu N \to eX$) processes, respectively. In the last term, the $-$ sign is taken for an incoming e^+ or $\bar{\nu}$ and the $+$ sign for an incoming e^- or ν. The factor $\eta^{\mathrm{NC}} = 1$ for unpolarized $e^\pm$ beams, whereas*

$$
\eta^{\mathrm{CC}} = (1 \pm \lambda)^2 \eta_W \tag{16.9}
$$

with $\pm$ for $\ell^\pm$ and where λ is the helicity of the incoming lepton. η_W is defined in Eq. (16.4). The CC structure functions, which derive exclusively from W exchange, are

$$
F_1^{\mathrm{CC}} = F_1^W, \; F_2^{\mathrm{CC}} = F_2^W, \; x F_3^{\mathrm{CC}} = x F_3^W . \tag{16.10}
$$

The NC structure functions $F_2^\gamma, F_2^{\gamma Z}, F_2^Z$ are, for $e^\pm N \to e^\pm X$, given by Ref. 5,

$$F_2^{\text{NC}} = F_2^\gamma - (g_V^e \pm \lambda g_A^e)\eta_{\gamma Z} F_2^{\gamma Z} + (g_V^{e\,2} + g_A^{e\,2} \pm 2\lambda g_V^e g_A^e)\,\eta_Z F_2^Z \qquad (16.11)$$

and similarly for F_1^{NC}, whereas

$$xF_3^{\text{NC}} = -(g_A^e \pm \lambda g_V^e)\eta_{\gamma Z} xF_3^{\gamma Z} + [2g_V^e g_A^e \pm \lambda(g_V^{e\,2} + g_A^{e\,2})]\eta_Z xF_3^Z . \qquad (16.12)$$

The polarized cross-section difference

$$\Delta\sigma = \sigma(\lambda_n = -1, \lambda_\ell) - \sigma(\lambda_n = 1, \lambda_\ell) , \qquad (16.13)$$

where λ_ℓ, λ_n are the helicities (± 1) of the incoming lepton and nucleon, respectively, may be expressed in terms of the five structure functions $g_{1,...5}(x, Q^2)$ of Eq. (16.6). Thus,

$$
\begin{aligned}
\frac{d^2\Delta\sigma^i}{dxdy} =\ & \frac{8\pi\alpha^2}{xyQ^2}\,\eta^i \left\{ -\lambda_\ell y \left(2 - y - 2x^2 y^2 \frac{M^2}{Q^2}\right) xg_1^i + \lambda_\ell 4x^3 y^2\,\frac{M^2}{Q^2}\,g_2^i \right. \\
& + 2x^2 y \frac{M^2}{Q^2} \left(1 - y - x^2 y^2 \frac{M^2}{Q^2}\right) g_3^i \\
& \left. - \left(1 + 2x^2 y \frac{M^2}{Q^2}\right) \left[\left(1 - y - x^2 y^2 \frac{M^2}{Q^2}\right) g_4^i + xy^2 g_5^i\right] \right\}
\end{aligned}
\qquad (16.14)
$$

with $i = \text{NC}$ or CC as before. The Eq. (16.13) corresponds to the difference of antiparallel minus parallel spins of the incoming particles for e^- or ν initiated reactions, but parallel minus antiparallel for e^+ or $\bar\nu$ initiated processes. For longitudinal nucleon polarization, the contributions of g_2 and g_3 are suppressed by powers of M^2/Q^2. These structure functions give an unsuppressed contribution to the cross section for transverse polarization [1], but in this case the cross-section difference vanishes as $M/Q \to 0$.

Because the same tensor structure occurs in the spin-dependent and spin-independent parts of the hadronic tensor of Eq. (16.6) in the $M^2/Q^2 \to 0$ limit, the differential cross-section difference of Eq. (16.14) may be obtained from the differential cross section Eq. (16.8) by replacing

$$F_1 \to -g_5 , \quad F_2 \to -g_4 , \quad F_3 \to 2g_1 , \qquad (16.15)$$

and multiplying by two, since the total cross section is the average over the initial-state polarizations. In this limit, Eq. (16.8) and Eq. (16.14) may be written in the form

$$\frac{d^2\sigma^i}{dxdy} = \frac{2\pi\alpha^2}{xyQ^2}\,\eta^i \left[Y_+ F_2^i \mp Y_- xF_3^i - y^2 F_L^i\right],$$

$$\frac{d^2\Delta\sigma^i}{dxdy} = \frac{4\pi\alpha^2}{xyQ^2}\,\eta^i \left[-Y_+ g_4^i \mp Y_- 2xg_1^i + y^2 g_L^i\right], \qquad (16.16)$$

with $i = $ NC or CC, where $Y_\pm = 1 \pm (1 - y)^2$ and

$$F_L^i = F_2^i - 2xF_1^i , \qquad g_L^i = g_4^i - 2xg_5^i . \tag{16.17}$$

In the naive quark-parton model, the analogy with the Callan-Gross relations [6] $F_L^i = 0$, are the Dicus relations [7] $g_L^i = 0$. Therefore, there are only two independent polarized structure functions: g_1 (parity conserving) and g_5 (parity violating), in analogy with the unpolarized structure functions F_1 and F_3.

16.2.1.   *Structure functions in the quark-parton model*:

In the quark-parton model [8,9], contributions to the structure functions F^i and g^i can be expressed in terms of the quark distribution functions $q(x, Q^2)$ of the proton, where $q = u, \overline{u}, d, \overline{d}$ etc. The quantity $q(x, Q^2)dx$ is the number of quarks (or antiquarks) of designated flavor that carry a momentum fraction between x and $x + dx$ of the proton's momentum in a frame in which the proton momentum is large.

For the neutral-current processes $ep \to eX$,

$$\left[F_2^\gamma, \ F_2^{\gamma Z}, \ F_2^Z\right] = x \sum_q \left[e_q^2, \ 2e_q g_V^q, \ g_V^{q\,2} + g_A^{q\,2}\right] (q + \overline{q}) ,$$

$$\left[F_3^\gamma, \ F_3^{\gamma Z}, \ F_3^Z\right] = \sum_q \left[0, \ 2e_q g_A^q, \ 2g_V^q g_A^q\right] (q - \overline{q}) ,$$

$$\left[g_1^\gamma, \ g_1^{\gamma Z}, \ g_1^Z\right] = \tfrac{1}{2} \sum_q \left[e_q^2, \ 2e_q g_V^q, \ g_V^{q\,2} + g_A^{q\,2}\right] (\Delta q + \Delta \overline{q}) ,$$

$$\left[g_5^\gamma, \ g_5^{\gamma Z}, \ g_5^Z\right] = \sum_q \left[0, \ e_q g_A^q, \ g_V^q g_A^q\right] (\Delta q - \Delta \overline{q}) , \tag{16.18}$$

where $g_V^q = \pm\tfrac{1}{2} - 2e_q \sin^2 \theta_W$ and $g_A^q = \pm\tfrac{1}{2}$, with $\pm$ according to whether q is a $u-$ or $d-$type quark respectively. The quantity Δq is the difference $q\!\uparrow -q\!\downarrow$ of the distributions with the quark spin parallel and antiparallel to the proton spin.

For the charged-current processes $e^- p \to \nu X$ and $\overline{\nu} p \to e^+ X$, the structure functions are:

$$F_2^{W^-} = 2x(u + \overline{d} + \overline{s} + c\ldots) ,$$
$$F_3^{W^-} = 2(u - \overline{d} - \overline{s} + c\ldots) ,$$
$$g_1^{W^-} = (\Delta u + \Delta \overline{d} + \Delta \overline{s} + \Delta c\ldots) ,$$
$$g_5^{W^-} = (-\Delta u + \Delta \overline{d} + \Delta \overline{s} - \Delta c\ldots) , \tag{16.19}$$

where only the active flavors are to be kept and where CKM mixing has been neglected. For $e^+ p \to \overline{\nu} X$ and $\nu p \to e^- X$, the structure functions F^{W^+}, g^{W^+} are obtained by

the flavor interchanges $d \leftrightarrow u, s \leftrightarrow c$ in the expressions for F^{W^-}, g^{W^-}. The structure functions for scattering on a neutron are obtained from those of the proton by the interchange $u \leftrightarrow d$. For both the neutral and charged-current processes, the quark-parton model predicts $2xF_1^i = F_2^i$ and $g_4^i = 2xg_5^i$.

Neglecting masses, the structure functions g_2 and g_3 contribute only to scattering from transversely polarized nucleons (for which $S \cdot q = 0$), and have no simple interpretation in terms of the quark-parton model. They arise from off-diagonal matrix elements $\langle P, \lambda'|[J_\mu^\dagger(z), J_\nu(0)]|P, \lambda\rangle$, where the proton helicities satisfy $\lambda' \neq \lambda$. In fact, the leading-twist contributions to both g_2 and g_3 are both twist-2 and twist-3, which contribute at the same order of Q^2. The Wandzura-Wilczek relation [10] expresses the twist-2 part of g_2 in terms of g_1 as

$$g_2^i(x) \; = \; -g_1^i(x) \; + \; \int_x^1 \frac{dy}{y} \, g_1^i(y) \; . \tag{16.20}$$

However, the twist-3 component of g_2 is unknown. Similarly, there is a relation expressing the twist-2 part of g_3 in terms of g_4. A complete set of relations, including M^2/Q^2 effects, can be found in Ref. 11.

16.2.2.   *Structure functions and QCD*:

One of the most striking predictions of the quark-parton model is that the structure functions F^i, g^i *scale*, *i.e.*, $F^i(x, Q^2) \rightarrow F^i(x)$ in the Bjorken limit that Q^2 and $\nu \rightarrow \infty$ with x fixed [12]. This property is related to the assumption that the transverse momentum of the partons in the infinite-momentum frame of the proton is small. In QCD, however, the radiation of hard gluons from the quarks violates this assumption, leading to logarithmic scaling violations, which are particularly large at small x, see Fig. 16.2. The radiation of gluons produces the evolution of both the structure functions and the parton distribution functions. As Q^2 increases, more and more gluons are radiated, which in turn split into $q\bar{q}$ pairs. This process leads both to the softening of the initial quark momentum distributions and to the growth of the gluon density and the $q\bar{q}$ sea as x decreases.

In QCD, the above process is described in terms of scale-dependent parton distributions $f(x, \mu^2)$, where $f = g$ or q and, typically, μ is the scale of the probe Q. These distributions correspond, at a given x, to the density of partons in the proton integrated over transverse momentum k_t up to μ. Their evolution in μ is described in QCD by the DGLAP equations (see Refs. 14–17) which have the schematic form

$$\frac{\partial f}{\partial \ln \mu^2} \sim \frac{\alpha_s(\mu^2)}{2\pi} \, (P \otimes f) \; , \tag{16.21}$$

where $\otimes$ denotes the convolution integral

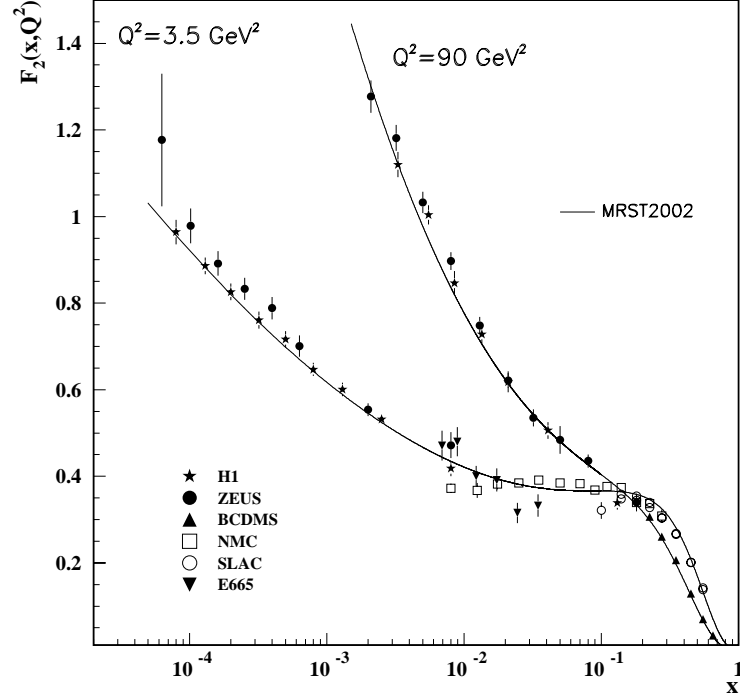$$P \; \otimes \; f \; = \; \int_x^1 \frac{dy}{y} \, P(y) \, f\left(\frac{x}{y}\right) \; . \tag{16.22}$$

Figure 16.2: The proton structure function F_2^p given at two Q^2 values (3.5 GeV^2 and 90 GeV^2), which exhibit scaling at the 'pivot' point $x \sim 0.14$. See the caption in Fig. 16.6 for the references of the data. Also shown is the MRST2002 parameterization [13] given at the same scales.

Although perturbative QCD can predict, via Eq. (16.21), the evolution of the parton distribution functions from a particular scale, μ_0, it cannot predict them *a priori* at any particular μ_0. Thus they must be measured at a starting point μ_0 before the predictions of QCD can be compared to the data at other scales, μ. In general, all observables involving a hard hadronic interaction (such as structure functions) can be expressed as a convolution of calculable, process-dependent coefficient functions and these universal parton distributions.

It is often convenient to write the evolution equations in terms of the gluon, non-singlet (q^{NS}) and singlet (q^S) quark distributions, such that

$$q^{NS} = q_i - \overline{q}_i, \qquad q^S = \sum_i (q_i + \overline{q}_i) . \tag{16.23}$$

The non-singlet distributions have non-zero values of flavor quantum numbers, such as isospin and baryon number. The DGLAP evolution equations then take the form

$$\frac{\partial q^{NS}}{\partial \ln \mu^2} = \frac{\alpha_s(\mu^2)}{2\pi} \, P_{qq} \, \otimes \, q^{NS} ,$$

$$\frac{\partial}{\partial \ln \mu^2} \begin{pmatrix} q^S \\ g \end{pmatrix} = \frac{\alpha_s(\mu^2)}{2\pi} \begin{pmatrix} P_{qq} & 2n_f \, P_{qg} \\ P_{gq} & P_{gg} \end{pmatrix} \otimes \begin{pmatrix} q^S \\ g \end{pmatrix} , \tag{16.24}$$

where P are splitting functions that describe the probability of a given parton splitting into two others, and n_f is the number of (active) quark flavors. The leading-order Altarelli-Parisi [16] splitting functions are

$$P_{qq} = \frac{4}{3} \left[\frac{1 + x^2}{(1 - x)} \right]_+ = \frac{4}{3} \left[\frac{1 + x^2}{(1 - x)_+} \right] + 2\delta(1 - x) , \tag{16.25}$$

$$P_{qg} = \frac{1}{2} \left[x^2 + (1 - x)^2 \right] , \tag{16.26}$$

$$P_{gq} = \frac{4}{3} \left[\frac{1 + (1 - x)^2}{x} \right] , \tag{16.27}$$

$$P_{gg} = 6 \left[\frac{1 - x}{x} + x(1 - x) + \frac{x}{(1 - x)_+} \right]$$
$$+ \left[\frac{11}{2} - \frac{n_f}{3} \right] \delta(1 - x), \tag{16.28}$$

where the notation $[F(x)]_+$ defines a distribution such that for any sufficiently regular test function, $f(x)$,

$$\int_0^1 dx \, f(x) [F(x)]_+ = \int_0^1 dx \, (f(x) - f(1)) F(x) . \tag{16.29}$$

In general, the structure functions can be expressed as a power series in α_s. The series contains both terms proportional to $\ln \mu^2$ and to $\ln 1/x$. The leading $\ln \mu^2$ terms come, in an axial gauge, from evolution along the parton chain that is strongly ordered in transverse momenta, that is $\mu^2 \gg k_{t,n}^2 \gg k_{t,n-1}^2 \gg \ldots$, where n denotes the nth parton-branching process and k_t the parton transverse momentum. The leading-order DGLAP evolution sums up the $(\alpha_s \ln \mu^2)^n$ contributions. The next-to-leading order (NLO) sums up the $\alpha_s(\alpha_s \ln \mu^2)^{n-1}$ terms [18,19], which arise when two adjacent $k_{t,i}$'s are no longer strongly ordered but become comparable, thereby losing a factor of $\ln \mu^2$. The NNLO contributions are now almost all known (see Refs. 20–24).

In the small x kinematic region, it is essential to sum leading terms in $\ln 1/x$, independent of the value of $\ln \mu^2$. At leading order, this is done by the BFKL equation for the unintegrated distributions (see Refs. 25,26). The leading-order $(\alpha_s \ln(1/x))^n$ terms come from the configuration strongly ordered in x, *i.e.*, $x \ll x_n \ll x_{n-1} \ll \ldots$.

In general, however, QCD color coherence implies *angular* ordering along the chain, so that it is necessary to work in terms of $f_a(x, k_t^2, \mu^2)$, the parton distributions unintegrated over k_t. These distributions depend on two hard scales: k_t and the scale μ of the probe. Consequently they satisfy more complicated CCFM evolution equations [27,28]. The DGLAP and BFKL equations are two limits of angular-ordered evolution. In the DGLAP

collinear approximation, the angle increases due to the growth of k_t, while, in the BFKL treatment, the angle ($\theta \simeq k_t/k_l$, where k_l is the longitudinal momentum) grows due to the decrease of the longitudinal-momentum fraction, x, along the chain of parton emissions from the proton.

As yet, there is no firm evidence in the data for $Q^2 \gtrsim 2$ GeV^2 for any deviation from standard DGLAP evolution, except that some DGLAP parton sets predict an unphysical behavior for F_L at low x [29], see however Ref. 30.

The precision of the contemporary experimental data demands that NLO (or even NNLO) DGLAP evolution be used in comparisons between QCD theory and experiment. At higher orders, it is necessary to specify, and to use consistently, both a renormalization and a factorization scheme. Whereas the renormalization scheme used is almost universally the modified minimal subtraction ($\overline{MS}$) scheme, there are two popular choices for factorization scheme, in which the form of the correction for each structure function is different. The two most-used factorization schemes are: DIS [31], in which there are no higher-order corrections to the F_2 structure function, and $\overline{MS}$ (based on Refs. 32–34). They differ by how the higher-order gluon divergences are assimilated in the parton distribution functions.

Perturbative QCD predicts the Q^2 behavior of leading-twist (twist-2) contributions to the structure functions. Higher-twist terms, which involve their own non-perturbative input, can occur. These die off as powers of Q; specifically twist-n terms are damped by $1/Q^{n-2}$. The higher-twist terms appear to be numerically unimportant for Q^2 above a few GeV^2, except for x close to 1. At very large values of x, perturbative corrections proportional to $\log(1-x)$ can become important [35].

So far, it has been assumed that the quarks are massless. The effects of the c and b-quark masses on the evolution have been studied, for example, in Refs. 36–39. An approach using a variable flavor number is now generally adopted, in which evolution with $n_f = 3$ is matched to that with $n_f = 4$ at the charm threshold, with an analogous matching at the bottom threshold.

16.3. Determination of parton distributions

The parton distribution functions (PDFs) can be determined from data for deep inelastic lepton-nucleon scattering and for related hard-scattering processes initiated by nucleons. Table 16.1 given below (based on Ref. 40) highlights some processes and their primary sensitivity to PDFs.

The kinematic ranges of fixed-target and collider experiments are complementary (as is shown in Fig. 16.3) which enables the determination of PDFs over a wide range in x and Q^2. Recent determinations of the unpolarized PDF's from NLO global analyses are given in Refs. 29,13 and Ref. 41, and at NNLO in Refs. 42,30, see also Ref. 43. Recent studies of the uncertainties in the PDFs and observables can be found in Refs. 44,45 and Refs. 13,30, see also Ref. 46. The result of one analysis is shown in Fig. 16.4 at a scale $\mu^2 = 10$ GeV^2. The polarized PDFs are obtained through NLO global analyses of measurements of the g_1 structure function in inclusive polarized deep inelastic scattering (for recent examples see Refs. 47–49). The inclusive data do not provide enough observables to determine

Table 16.1: Lepton-nucleon and related hard-scattering processes and their primary sensitivity to the parton distributions that are probed.

Process	Main Subprocess	PDFs Probed
$\ell^{\pm}N \to \ell^{\pm}X$	$\gamma^* q \to q$	$g(x \lesssim 0.01), q, \overline{q}$
$\ell^+(\ell^-)N \to \overline{\nu}(\nu)X$	$W^* q \to q'$	
$\nu(\overline{\nu})N \to \ell^-(\ell^+)X$	$W^* q \to q'$	
$\nu\, N \to \mu^+\mu^- X$	$W^* s \to c \to \mu^+$	s
$pp \to \gamma X$	$qg \to \gamma q$	$g(x \sim 0.4)$
$pN \to \mu^+\mu^- X$	$q\overline{q} \to \gamma^*$	$\overline{q}$
$pp, pn \to \mu^+\mu^- X$	$u\overline{u}, d\overline{d} \to \gamma^*$	$\overline{u} - \overline{d}$
	$u\overline{d}, d\overline{u} \to \gamma^*$	
$ep, en \to e\pi X$	$\gamma^* q \to q$	
$p\overline{p} \to W \to \ell^{\pm}X$	$ud \to W$	$u, d, u/d$
$p\overline{p} \to$ jet $+X$	$gg, qg, qq \to 2j$	$q, g(0.01 \lesssim x \lesssim 0.5)$

all polarized PDFs. These polarized PDFs may be fully accessed via flavor tagging in semi-inclusive deep inelastic scattering. Fig. 16.5 shows several global analyses at a scale of 2.5 GeV^2 along with the data from semi-inclusive DIS.
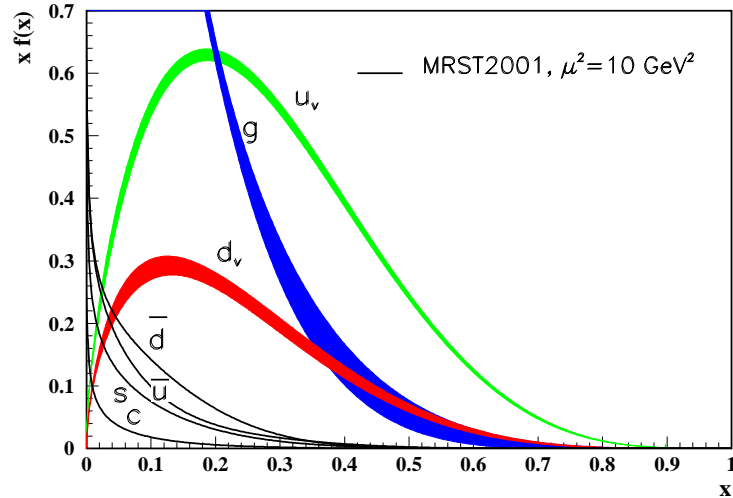

Figure 16.4: Distributions of x times the unpolarized parton distributions $f(x)$ (where $f = u_v, d_v, \overline{u}, \overline{d}, s, c, g$) using the MRST2001 parameterization [29,13] (with uncertainties for u_v, d_v, and g) at a scale $\mu^2 = 10$ GeV^2.
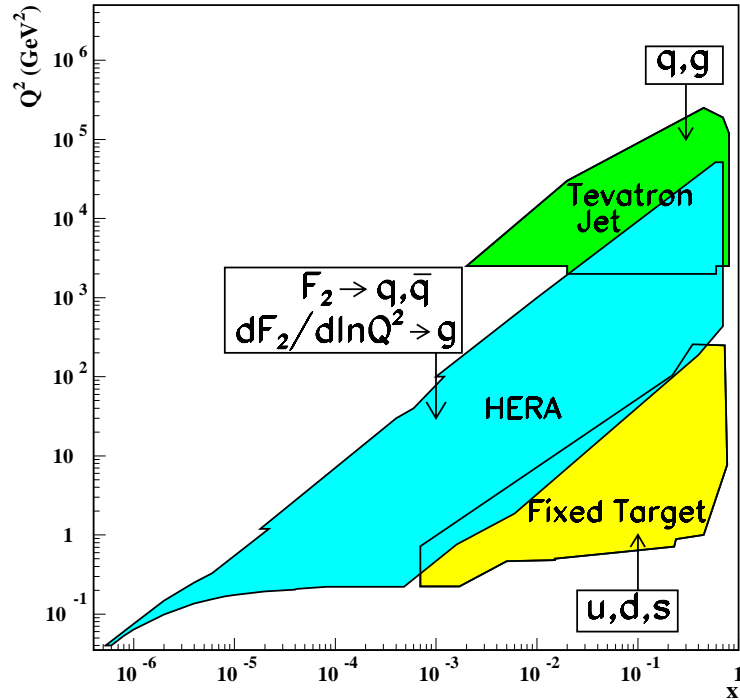
Figure 16.3: Kinematic domains in x and Q^2 probed by fixed-target and collider experiments, shown together with the important constraints they make on the various parton distributions.

Comprehensive sets of PDFs available as program-callable functions can be obtained from several sources *e.g.*, Refs. 52,53. As a result of a Les Houches Accord, a PDF package (LHAPDF) exists [54] which facilitates the inclusion of recent PDFs in Monte Carlo/Matrix Element programs in a very compact and efficient format.
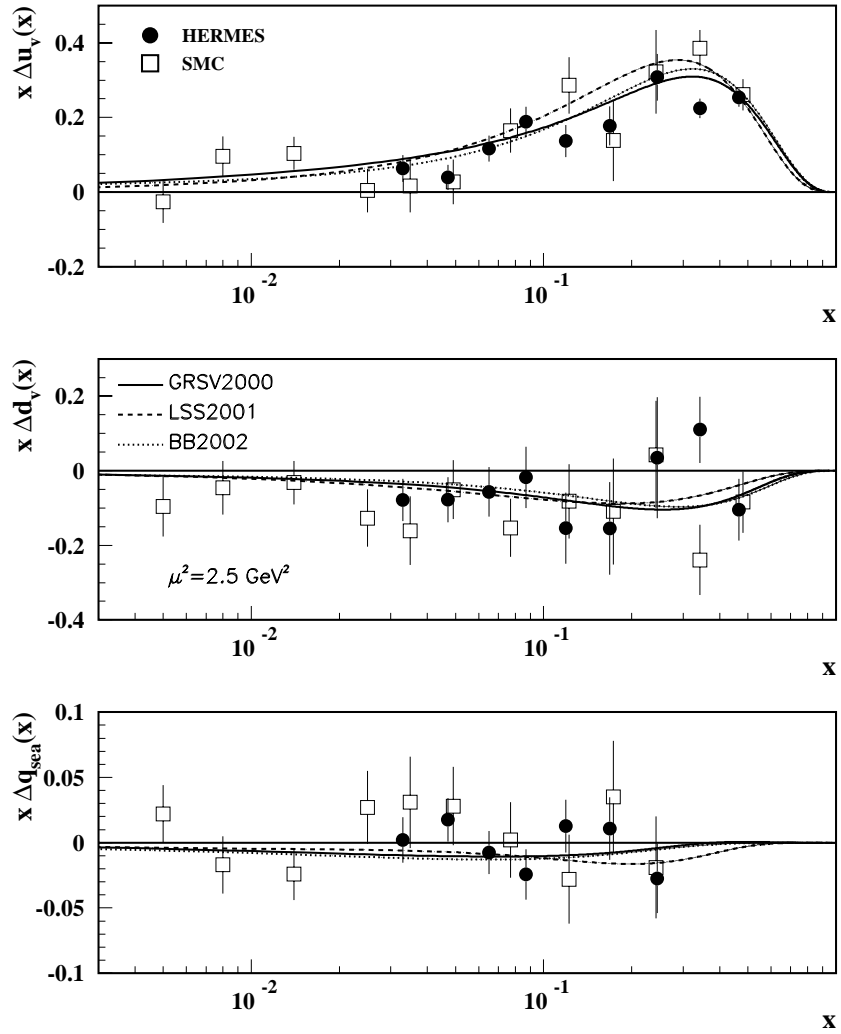
Figure 16.5: Distributions of x times the polarized parton distributions $\Delta q(x)$ (where $q = u_v, d_v, q_{sea}$) using the GRSV2000 [47], LSS2001 [48], and BB2002 [49] parameterizations at a scale $\mu^2 = 2.5$ GeV^2. Points represent data from semi-inclusive positron (HERMES [50]) and muon (SMC [51]) deep inelastic scattering given at $Q^2 = 2.5$ GeV^2.

16.4. DIS determinations of α_s

Table 16.2 shows the values of $\alpha_S(M_Z^2)$ found in recent fits to DIS and related data in which the coupling is left as a free parameter.

Table 16.2: The values of $\alpha_S(M_Z^2)$ found in NLO and NNLO fits to DIS data. The experimental errors quoted correspond to an increase $\Delta\chi^2$ from the best fit value of χ^2. CTEQ6 [41] and MRST03 [30] are global fits. H1 [56] fit only a subset of the F_2^{ep} data, while Alekhin [43] also includes F_2^{ed} and ZEUS [55] in addition include xF_3^ν data.

	$\Delta\chi^2$	$\alpha_S(M_Z^2) \ \pm\,\text{expt} \pm \text{theory} \pm \text{model}$
NLO		
CTEQ6	100	0.1165 ± 0.0065
ZEUS	50	$0.1166 \pm 0.0049 \qquad\qquad \pm 0.0018$
MRST03	5	$0.1165 \pm 0.002 \ \pm 0.003$
H1	1	$0.115 \ \ \pm 0.0017 \pm 0.005^{+0.0009}_{-0.0005}$
Alekhin	1	$0.1171 \pm 0.0015 \pm 0.0033$
NNLO		
MRST03	5	$0.1153 \pm 0.002 \pm 0.003$
Alekhin	1	$0.1143 \pm 0.0014 \pm 0.0009$

There have been several other studies of α_s at NNLO, and beyond, using subsets of DIS data (see, for example, Refs. 57–59). Moreover, there exist global NLO analyses of polarised DIS data which give $\alpha_s(M_Z^2) = 0.120 \pm 0.009$ [60] and 0.114 ± 0.009 [49].

16.5. The hadronic structure of the photon

Besides the *direct* interactions of the photon, it is possible for it to fluctuate into a hadronic state via the process $\gamma \to q\overline{q}$. While in this state, the partonic content of the photon may be *resolved*, for example, through the process $e^+e^- \to e^+e^-\gamma^*\gamma \to e^+e^-X$ where the virtual photon emitted by the deep inelastic scattering lepton probes the hadronic structure of the quasi-real photon emitted by the other lepton. The perturbative LO contributions, $\gamma \to q\overline{q}$ followed by $\gamma^*q \to q$, are subject to QCD corrections due to the coupling of quarks to gluons.

Often the equivalent-photon approximation is used to express the differential cross section for deep inelastic electron–photon scattering in terms of the structure functions of the transverse quasi-real photon times a flux factor N for the incoming quasi-real photons of transverse polarisation

$$\frac{d^2\sigma}{dxdQ^2} = N\frac{2\pi\alpha^2}{xQ^4}\left[\left(1 + (1-y)^2\right)F_2^\gamma(x, Q^2) - y^2F_L^\gamma(x, Q^2)\right],$$

where we have used $F_2^\gamma = 2xF_T^\gamma + F_L^\gamma$. Complete formulae are given, for example, in the comprehensive review of Ref. 61.

The hadronic photon structure function F_2^γ evolves from the 'hadron-like' behavior, calculable via the vector-meson-dominance model, to the dominating 'point-like' behaviour, calculable in perturbative QCD, with increasing Q^2. Due to the point-like coupling, the logarithmic evolution of F_2^γ with Q^2 has a *positive* slope for all values of x, see Fig. 16.13. The 'loss' of quarks at large x due to gluon radiation is over-compensated by the 'creation' of quarks via the point-like $\gamma \to q\bar{q}$ coupling. The logarithmic evolution was first predicted in the quark–parton model ($\gamma^*\gamma \to q\bar{q}$) [62,63] and then in QCD in the limit of large Q^2 [64].

---

* The value of η^{CC} deduced from Ref. 1 is found to be a factor of two too small; η^{CC} of Eq. (16.9) agrees with Refs. 2,3.

References:

1.   J. Blümlein and N. Kochelev, Nucl. Phys. **B498**, 285 (1997).
2.   S. Forte, M.L. Mangano, and G. Ridolfi, Nucl. Phys. **B602**, 585 (2001).
3.   M. Anselmino, P. Gambino, and J. Kalinowski, Z. Phys. **C64**, 267 (1994).
4.   M. Anselmino, A. Efremov, and E. Leader, Phys. Rep. **261**, 1 (1995).
5.   M. Klein and T. Riemann, Z. Phys. **C24**, 151 (1984).
6.   C.G. Callan and D.J. Gross, Phys. Rev. Lett. **22**, 156 (1969).
7.   D.A. Dicus, Phys. Rev. **D5**, 1367 (1972).
8.   J.D. Bjorken and E.A. Paschos, Phys. Rev. **185**, 1975 (1969).
9.   R.P. Feynman, Photon Hadron Interactions (Benjamin, New York, 1972).
10.   S. Wandzura and F. Wilczek, Phys. Rev. **B72**, 195 (1977).
11.   J. Blümlein and A. Tkabladze, Nucl. Phys. **B553**, 427 (1999).
12.   J.D. Bjorken, Phys. Rev. **179**, 1547 (1969).
13.   A.D. Martin, R.G. Roberts, W.J. Stirling, and R.S. Thorne, Eur. Phys. J. **C28**, 455 (2003).
14.   V.N. Gribov and L.N. Lipatov, Sov. J. Nucl. Phys. **15**, 438 (1972).
15.   L.N. Lipatov, Sov. J. Nucl. Phys. **20**, 95 (1975).
16.   G. Altarelli and G. Parisi, Nucl. Phys. **B126**, 298 (1977).
17.   Yu.L. Dokshitzer, Sov. Phys. JETP **46**, 641 (1977).
18.   G. Curci, W. Furmanski, and R. Petronzio, Nucl. Phys. **B175**, 27 (1980).
19.   R.K. Ellis, W.J. Stirling, and B.R. Webber, QCD and Collider Physics (Cambridge UP, 1996).
20.   E.B. Zijlstra and W.L. van Neerven, Nucl. Phys. **B383**, 525 (1992).
21.   S. Moch and J.A.M. Vermaseren, Nucl. Phys. **B573**, 853 (2000).
22.   S.A. Larin, P. Nogueira, T. van Ritbergen and J.A.M. Vermaseren, Nucl. Phys. **B492**, 338 (1997).
23.   A. Retey and J.A.M. Vermaseren, Nucl. Phys. **B604**, 281 (2001).

24. S. Moch, J.A.M. Vermaseren and A. Vogt, Nucl. Phys. **B646**, 181 (2002).

25. E.A. Kuraev, L.N. Lipatov, and V.S. Fadin, Phys. Lett. **B60**, 50 (1975); Sov. Phys. JETP **44**, 443 (1976); Sov. Phys. JETP **45**, 199 (1977).

26. Ya.Ya. Balitsky and L.N. Lipatov, Sov. J. Nucl. Phys. **28**, 822 (1978).

27. M. Ciafaloni, Nucl. Phys. **B296**, 49 (1988).

28. S. Catani, F. Fiorani, and G. Marchesini, Phys. Lett. **B234**, 339 (1990); Nucl. Phys. **B336**, 18 (1990).

29. A.D. Martin, R.G. Roberts, W.J. Stirling, and R.S. Thorne, Eur. Phys. J. **C23**, 73 (2002).

30. A.D. Martin, R.G. Roberts, W.J. Stirling and R.S. Thorne, (MRST2003) `hep-ph/0308087`.

31. G. Altarelli, R.K. Ellis, and G. Martinelli, Nucl. Phys. **B143**, 521 (1978) and erratum: Nucl. Phys. **B146**, 544 (1978).

32. G. 't Hooft and M. Veltman, Nucl. Phys. **B44**, 189 (1972).

33. G. 't Hooft, Nucl. Phys. **B61**, 455 (1973).

34. W.A. Bardeen *et al.*, Phys. Rev. **D18**, 3998 (1978).

35. G. Sterman, Nucl. Phys. **B281**, 310 (1987).

36. M.A.G. Aivazis *et al.*, Phys. Rev. **D50**, 3102 (1994).

37. J.C. Collins, Phys. Rev. **D58**, 094002 (1998).

38. R.S. Thorne and R.G. Roberts, Phys. Rev. **D57**, 1998 (1998); Phys. Lett. **B421**, 303 (1998); Eur. Phys. J. **C19**, 339 (2001).

39. W.-K. Tung, S. Kretzer and C. Schmidt, J. Phys. **G28**, 983 (2002).

40. A.D. Martin, R.G. Roberts, W.J. Stirling, and R.S. Thorne, Eur. Phys. J. **C4**, 463 (1998).

41. CTEQ, J. Pumplin *et al.*, JHEP **0207**, 012 (2002).

42. A.D. Martin, R.G. Roberts, W.J. Stirling, and R.S. Thorne, Phys. Lett. **B531**, 216 (2002).

43. S. Alekhin, JHEP **0302**, 015 (2003).

44. CTEQ, D. Stump *et al.*, Phys. Rev. **D65**, 014012 (2001).

45. CTEQ, J. Pumplin *et al.*, Phys. Rev. **D65**, 014013 (2001).

46. W.T. Giele, S. Keller and D.A. Kosower, `hep-ph/0104052`.

47. M. Glück, E. Reya, M. Stratmann, and W. Vogelsang, Phys. Rev. **D63**, 094005 (2001).

48. E. Leader, A.V. Sidorov and D.B. Stamenov, Eur. Phys. J. **C23**, 479 (2002).

49. J. Blümlein and H. Böttcher, Nucl. Phys. **B636**, 225 (2002).

50. HERMES, K. Ackerstaff *et al.*, Phys. Lett. **B464**, 123 (1999).

51. SMC, B. Adeva *et al.*, Phys. Lett. **B420**, 180 (1998).

52. H. Plothow-Besch, CERN PDFLIB, W5051 (2000).

53. `http://durpdg.dur.ac.uk/HEPDATA/PDF`.

54. http://durpdg.dur.ac.uk/lhapdf/index.html.

55. ZEUS, S. Chenakov *et al.*, Phys. Rev. **D67**, 012007 (2003).

56. H1, C. Adloff *et al.*, Eur. Phys. J. **C21**, 33 (2001).

57. W.L. van Neerven and A. Vogt, Nucl. Phys. **B603**, 42 (2001).

58. J. Santiago and F.J. Yndurain, Nucl. Phys. **B611**, 447 (2001).

59. A.L. Kataev, G. Parente, and A.V. Sidorov, Nucl. Phys. Proc. Supp. **116**, 105 (2003).

60. G. Altarelli, R.D. Ball, S. Forte, and G. Ridolfi, Nucl. Phys. **B496**, 337 (1997).

61. R. Nisius, Phys. Reports **332**, 165 (2000).

62. T.F. Walsh and P.M. Zerwas, Phys. Lett. **B44**, 195 (1973).

63. R.L. Kingsley, Nucl. Phys. **B60**, 45 (1973).

64. E. Witten, Nucl. Phys. **B120**, 189 (1977).